Optical coherent transients and hole burning of the 7F0 - 5D0 transition in Eu(OH)3
by Michael Stephen Otteson

A thesis submitted in partial fulfillment of the requirements for the degree of Doctor of Philosophy i n Physics
Montana State University

Abstract:
The narrowest inhomogeneous optical linewidth ever seen in a solid has been observed in Eu(OH)^. This transition is quadratically enhanced in a magnetic field and the results are explained completely in terms of second order perturbation theory and the coupling of crystal field energy levels.

Optical coherent transients are reported here for the first time in this optically pure, stoichiometric material. The optical dephasing time, T2 is shown to be greater than 2 microseconds for the 7F0-5D0 zero phonon transition.

Hole burning, attributed to optical pumping of nuclear— qua drupole levels, has been used' to measure the qua drupole splittings in the excited, 5D0 , state. Due to the small magnetic moment, conventional magnetic resonance techniques have failed to make this measurement in all Europium compounds. The new technique developed and used in these hole burning measurements yields the quadrupole coupling coefficients, |P| = 11.6 MHz and |P| = 4.5 MHz for the 153 isotope and the 151 isotope, respectively.

The qualitative behavior of line narrowing in Doubly-resonant two—photon-absorption induced four—wave mixing is explained in terms of the anomalous dispersion. The implications of this dispersion regarding the measurement of the homogeneous linewidth and hyperfine levels hidden within the inhomogeneous profile are discussed with regard to the particular example of LiTbF4.

OPTICAL COHERENT TRANSIENTS AND HOLE BURNING OF THE $^7F_0$-$^5D_0$ TRANSITION IN $Eu(OH)_3$

by

Michael Stephen Otteson

A thesis submitted in partial fulfillment
of the requirements for the degree

of

Doctor of Philosophy

in

Physics

MONTANA STATE UNIVERSITY
Bozeman, Montana

November 1984

APPROVAL

of a thesis submitted by

Michael Stephen Otteson

This thesis has been read by each member of the thesis committee and has been found to be satisfactory regarding content, English usage, format, citations, bibliographic style, and consistency, and is ready for submission to the College of Graduate Studies.

11 November 1984
Date

Rufus L Cone
Chairperson, Graduate Committee

Approved for the Major Department

27 November 1984
Date

Robert J Iverson
Head, Major Department

Approved for the College of Graduate Studies

11-30-84
Date

Graduate Dean

STATEMENT OF PERMISSION TO USE

In presenting this thesis in partial fulfillment fo the requirements for a doctoral degree at Montana State University, I agree that the Library shall make it available to borrowers under rules of the Library. I further agree that copying of this thesis is allowable only for scholarly purposes, consistent with "fair use" as prescribed in the U.S. Copyright Law. Requests for extensive copying or reproduction of this thesis should be referred to University Microfilms International, 300 North Zeeb Road, Ann Arbor, Michigan 48106, to whom I have granted "the exclusive right to reproduce and distribute copies of the dissertation in and from microfilm and the right to reproduce and distribute by abstract in any format."

Signature Michael L. Otteson

Date November 30, 1984

VITA

Michael Stephen Otteson was born on April 3, 1951 in Stoughton, Wisconsin. He is the son of Otto C. and Jean M. Otteson.

Educated in the Wisconsin public school system, he graduated from Deerfield High School in 1969. He attended University of Wisconsin-Oshkosh and graduated with a B.S. degree in physics and applied mathematics in 1973 and the M.S. degree in 1976. He received the M.S. degree in physics from Montana State University in Bozeman, Montana in 1979.

ACKNOWLEDGEMENTS

The author wishes to acknowledge the contributions of several people to the preparation of this thesis. Foremost has been the encouragement and the assistance of his advisor, Dr. Rufus L. Cone, whose scientific guidance has been very helpful in this thesis and its preparation.

Thanks are also due to Mr. Al Beldring for his help and expertise in building electronic equipment; to Mr. Tom Jungst and Mr. Tony Knick in machining and building apparatus; and to Mr. Mark Baldwin for successfully supplying the liquid nitrogen needed in the experimental work.

The author also wishes to thank Dr. R. M. Macfarlane for many stimulating discussions and suggestions.

Finally, he wishes to extend a very warm thanks to his friend, Ms. Karen L. Thompson, for her help in preparing the manuscript, and to his parents for their encouraging support over the years.

TABLE OF CONTENTS

TABLE OF CONTENTS-continued

LIST OF TABLES

LIST OF FIGURES

LIST OF FIGURES-continued

LIST OF FIGURES-continued

Abstract

The narrowest inhomogeneous optical linewidth ever seen in a solid has been observed in $Eu(OH)_3$. This transition is quadratically enhanced in a magnetic field and the results are explained completely in terms of second order perturbation theory and the coupling of crystal field energy levels.

Optical coherent transients are reported here for the first time in this optically pure, stoichiometric material. The optical dephasing time, T_2, is shown to be greater than 2 microseconds for the $^7F_0-^5D_0$ zero phonon transition.

Hole burning, attributed to optical pumping of nuclear-quadrupole levels, has been used to measure the quadrupole splittings in the excited, $^5D_0$, state. Due to the small magnetic moment, conventional magnetic resonance techniques have failed to make this measurement in all Europium compounds. The new technique developed and used in these hole burning measurements yields the quadrupole coupling coefficients, $|P| = 11.6$ MHz and $|P| = 4.5$ MHz for the 153 isotope and the 151 isotope, respectively.

The qualitative behavior of line narrowing in Doubly-resonant two-photon-absorption induced four-wave mixing is explained in terms of the anomalous dispersion. The implications of this dispersion regarding the measurement of the homogeneous linewidth and hyperfine levels hidden within the inhomogeneous profile are discussed with regard to the particular example of $LiTbF_4$.

Chapter 1

INTRODUCTION

The rare earth ion, Eu^{3+}, exhibits several properties which make it interesting in a spectroscopic as well as a practical sense. The well established ground state[1] which is dominantly a $^7F_0$, J=0 state, is a nonmagnetic singlet electronic state. The singlet nature of the electronic state is also an attractive position from which to begin the study of higher order interactions such as the hyperfine structure. Because of the singlet electronic state the perturbations due to the crystal field can be described in a more straightforward manner.

In general, there is practical interest in trivalent rare earth ions for solid state lasers.[2] The rare earths have narrow emission and absorption linewidths and a quantum efficiency near 1.0 for some transitions. These features, and the fact that they can be easily incorporated into a variety of host lattices, make them very attractive as laser materials. The trivalent europium ion in a Y_2O_3[3] host lattice has displayed laser action. Absorption line- widths as small as 3.5 GHz have been measured in EuP_5O_{10}[4] at 1.6 K.

A general discussion of rare earth properties and some of the particular characteristics of the spectra are

presented in Chapter 2. This is followed by a description and explanation of two experimental techniques used in this study of $Eu(OH)_3$. Optical hole burning is explained in Chapter 3 and the measurement of optical dephasing using the new method of optical phase switching is explicated in chapter 4. Experimental details and the CW dye laser used in this study are described in chapter 5 before the discussion of results in chapter 6.

Initial interest in this work was stimulated by measurements of the optical linewidth of the $^7F_0 — ^5D_0$ transition in $Eu(OH)_3$. The measured value of 167 MHz full width at half maximum, FWHM, is the narrowest inhomogeneous width ever observed in any solid. In chapter 6 the experimental linewidth and shape of the absorption profile are discussed in detail along with the possibility of the first resolved optical isotope shift in a solid.

One of the major contributions of this work, is the added understanding of the dynamic change of the optical characteristics of $Eu(OH)_3$ and other Eu^{3+} compounds in an external magnetic field. The quadratic change in the oscillator strength and the small Zeeman shift are experimentally measured and explained in terms of second order perturbation theory in the second and third parts of Chapter 6 respectively.

The measurement of an optical dephasing time in $Eu(OH)_3$

is difficult because of the intrinsically small oscillator strength associated with the $^7F_0 \longleftrightarrow {}^5D_0$ transition in this material. The development of optical phase switching as a new technique for measuring coherent transients has renewed the interest in making measurements of this type in many different materials. A description of optical phase switching as an experimental method and the expected results of such a measurement are given in Chapter 4. The particular application of optical phase switching to measure the dephasing time in $Eu(OH)_3$ and conclusions concerning these measurements are discussed in part four of Chapter 6.

The use of spectral hole burning to measure nuclear hyperfine splittings has only recently been used to complement the results obtained by the use of the more standard nuclear magnetic resonance and nuclear quadrupole resonance techniques. In Chapter 3, an explanation of the hole burning process is presented with a discussion of some of the previous measurements. Measurement of the quadrupole coupling constants for each of the europium isotopes, and the new technique used to make these measurements in $Eu(OH)_3$ is described in detail in the last section of Chapter 6.

In Chapter 8 a new explanation is given for a particular type of four-wave mixing experiment along with the potential use of this type of experiment in measuring hyperfine splittings and homogeneous linewidths.

Chapter 2

RARE EARTH SPECTRA

Typically the spectrum of rare earth ions in a crystal consists of groups of lines; these groups are separated by approximately 1000 cm^{-1} and the sharp lines within a group are generally spread over an energy range of about 200 cm^{-1}. These groups are then labeled by the symbols of the dominant Russell-Saunders component. In fact, each group of states contains admixtures of states characterized by a set of quantum numbers S, L, J, yet for each group, J remains a relatively good quantum number.

The sharp absorption spectra of rare earth ions in ionic crystals were observed long ago.[5] In many cases these lines are as narrow as those observed in the spectra of free atoms or free molecules. This means widths of 0.01 Angstrom, or 3 GHz, occur in the spectra of these materials in solids at low temperature. These narrow spectral features exhibited by the rare earths imply that, in principle, it is possible to study optical interactions in a solid with an accuracy obtained with free atoms or ions.

The sharp spectra of the rare earth ions are a result of lanthanide contraction. The energy and spatial extension of the 4f eigenfunctions suddenly drops at the start of the

lanthanide series. The imperfect shielding of one 4f-electron by another 4f-electron also contributes to this contraction. As one proceeds through the series with each increase in nuclear charge and electron number, the effective nuclear charge increases, which causes a reduction of the entire $4f^n$ shell.[6] Because of this contraction the f-shell behaves as an inner shell and it is shielded by the outer $5s^2p^6$ closed shells of the xenon structure. As a consequence the rare earth ions do not interact appreciably with the environment and the 4f electrons have little tendency to participate in chemical bonding.

Free Ion

The electronic configuration of trivalent rare earth ions in a solid consists of the xenon structure of electrons with n electrons in the 4f shell, n=1 for cerium up to n=14 for lutecium. The Hamiltonian that determines the 4f energy levels of an isolated ion can be written as

$$H = (-\hbar^2/2m) \sum_{i=1} \nabla_i^2 - \sum_{i=1} Z^* e^2/r_i + \sum_{i<j} e^2/r_{ij} + \sum_{i=1} \xi(r_i) \vec{s}_i \cdot \vec{l}_i$$

where N is the number of electrons, Z^*e the screened charge of the nucleus, and $\xi(r_i)$ the spin-orbit coupling function.

The first two parts of the expression are spherically symmetric and therefore do not remove any of the

degeneracies of the 4f electrons. The last two terms, the mutual coulomb interaction and the spin-orbit interaction respectively, are responsible for the free ion energy level structure of the 4f electrons. Labeling these two terms as H_c for the coulomb interaction, and H_{so} for the spin-orbit interactions, there are two limiting cases to be considered. $H_c \gg H_{so}$ in which Russell-Saunders, or LS coupling applies, or $H_{so} \gg H_c$ in which the j-j coupling scheme can be used. The rare earths fit into neither of these cases, so the total Hamiltonian,

$$H_1 = H_c + H_{so},$$

must be diagonalized to determine the energy levels. This approach is called intermediate coupling and usually starts from a basis set of Russell-Saunders states. The general energy level diagram for trivalent europium, as determined by Dieke and Crosswhite,[7] is shown in Figure 1.

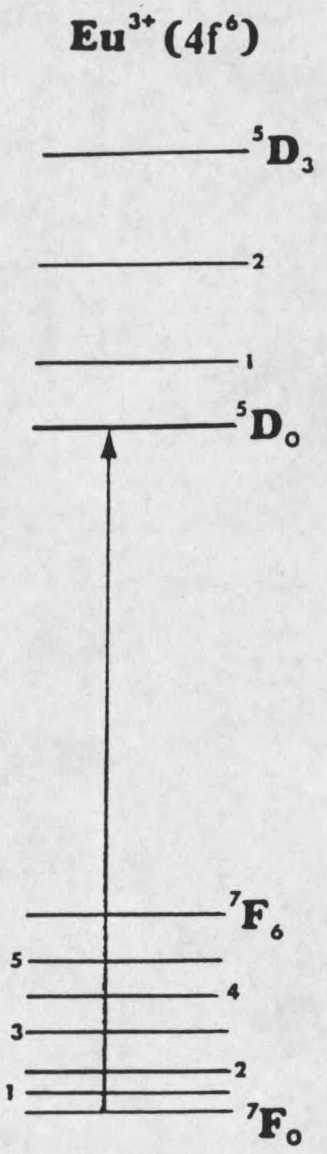

Figure 1: Energy level diagram for the trivalent rare earth ion Europium.

Crystal Field

When the ion is introduced into a crystal the ion experiences an inhomogeneous electric potential produced by the charge distribution in the crystal. Covalency and overlap effects also contribute to the potential. These effects are modeled by a one electron potential called the crystal field which removes some of the remaining degeneracy of the free ion. For rare earth ions, the splittings produced by the crystal field have been shown experimentally to be smaller than the energy separation of the free ion multiplets. So the crystal field splittings are obtained by treating the crystal field potential as a perturbation of the free ion.

The crystal field Hamiltonian is usually written as

$$V = \sum_{k,q,i} B_{kq} \, V_k^q \, (x_i, y_i, z_i)$$

where the parameters, B_{kq}, are treated as free parameters in fitting the crystal field energy levels. Before considering symmetry, as many as 27 complex constants would be needed to specify the crystal field potential. With time reversal symmetry this is reduced to 27 independent constants which must be real. The field for C_{3h} symmetry is specified by only four real parameters B_{20}, B_{40}, B_{60}, B_{66}, and the total Hamiltonian for equivalent f electrons can be written in the form[8]

$$H = H_0 + (B_{20}V_2^0 + B_{40}V_4^0 + B_{60}V_6^0 + B_{66}V_6^6)$$

where H_0 is the free ion Hamiltonian[9] and the V_k^q are polynomials of even degree.[10]

Matrix elements of the crystal field operators V_k^q can be calculated using spherical tensor operator methods and the doubly reduced matrix elements tabulated by Nielson and Koster.[11] Then the crystal field energies are obtained by using basis states corresponding to the free ion Hamiltonian, H_0, and diagonalizing the matrix of H on a computer.

$\underline{Eu^{3+}}$ $\underline{Ion}$ $\underline{in}$ $\underline{Eu(OH)_3}$

This was done for Eu^{3+} in $Eu(OH)_3$ by Cone and Faulhaber.[12] The fitted crystal field parameters are given by the following four constants.

$$B_{20} = 211 \pm 11 \text{ cm}^{-1} \qquad B_{40} = -71 \pm 8 \text{ cm}^{-1}$$

$$B_{60} = -54 \pm 3 \text{ cm}^{-1} \qquad B_{66} = 617 \pm 30 \text{ cm}^{-1}$$

In the paper by Cone and Faulhaber, absorption transitions between the ground state, $^7F_0$, and $^5D_0$, the lowest excited state in the D manifold were not reported because that transition is forbidden and very weak. But they were able to determine the position of the $^5D_0$ absorption by comparing the fluorescence from the $^5D_0$ state at 4.2K with the absorption from $^7F_1$ to $^5D_0$ at 77K to within an accuracy of about 1 cm^{-1}.

The energy level separations, from the paper by Cone

and Faulhaber[12], which will be necessary in later explanations of the phenomena observed in this crystal are given as follows.

$$^7F_0 \text{ — } ^7F_2 \quad \mu = 0 \quad = 1151 \text{ cm}^{-1}$$

$$^5D_0 \text{ — } ^5D_1 \quad \mu = 1 \quad = 1753 \text{ cm}^{-1}$$

$$^5D_0 \text{ — } ^5D_1 \quad \mu = 0 \quad = 1771 \text{ cm}^{-1}$$

$$^5D_0 \text{ — } ^5D_2 \quad \mu = 0 \quad = 4230 \text{ cm}^{-1}$$

The crystal field matrix elements must satisfy the selection rule $J_z - J'_z = q$. This implies a set of crystal quantum numbers μ may be introduced such that $J_z = \mu(\text{mod } q)$. These crystal quantum numbers are used to label the states given above. Also, complimenting these, are measurements made in this work corresponding to the energy level separations,

$$^7F_0 \text{ — } ^5D_0 \quad \mu = 0 \quad = 17226.8 \text{ cm}^{-1}$$

$$^7F_0 \text{ — } ^7F_1 \quad \mu = 1 \quad = 339 \text{ cm}^{-1}$$

$$^7F_0 \text{ — } ^7F_1 \quad \mu = 0 \quad = 440.5 \text{ cm}^{-1}$$

The energy differences, $^7F_0$—$^7F_1$ μ= 0, 1 and $^5D_0$—$^5D_1$ μ= 0, 1, will be used in the second section of chapter 6 to calculate the quadratic increase of the absorption coefficient as a function of the magnetic field. These energy level separations will also be used to calculate the observed Zeeman shift of the $^7F_0$ to $^5D_0$ transition which similarly varies with the square of the magnetic field strength.

In a calculation of the expected nuclear quadrupole

splittings, it is again necessary to use energy level separations. For this estimate, the difference energies of the $^7F_0$ — $^7F_2$ and $^5D_0$ — $^5D_2$ states are used in the calculation in Chapter 3. Although this calculation is just an estimate of the quadrupole splittings, it does reinforce the experimental results given in the last section of Chapter 6.

In itself, the existence of a transition between the $^7F_0$ ground state and the $^5D_0$ excited state is interesting because as pointed out by the Judd-Ofelt theory,[13] electric dipole transitions between the levels of the $4f^n$ configurations are all forbidden by the parity rule unless the $4f^n$ states have admixtures of opposite parity. The magnetic dipole selection rules are still valid in first order and explains the weak intensity for a J = 0 to J' = 0 transition. This transition in $Eu(OH)_3$ is magnetic dipole in character and consistent with the magnetic dipole selection rules given in Table 1 below.

Selection rules are of considerable importance, in all spectroscopic techniques for transitions between two energy levels, and selection rules in crystal spectra are directly connected with the symmetry of the crystal under consideration. The selection rules enable the experimenter to draw conclusions about the nature of the energy levels between which the transition takes place. The mathematical concept which deals with these symmetries is group theory.

Group theory as applied to rare earth crystal spectra was originally developed by Bethe,[14] but now it is readily available in tables for all of the different symmetries.[15] The selection rules for Eu^{3+}, with C_{3h} site symmetry,[16] in $Eu(OH)_3$ are shown in Table 1.

	μ'					
μ	0	3	-2	2	1	-1
0	mσ	eπ	eσ	eσ	mπ	mπ
3	eπ	mσ	mπ	mπ	eσ	eσ
-2	eσ	mπ	mσ	eσ	eπ	mπ
2	eσ	mπ	eσ	mσ	mπ	eπ
1	mπ	eσ	eπ	mπ	mσ	eσ
-1	mπ	eσ	mπ	eπ	eσ	mσ

Table I. Selection rules and crystal quantum numbers for even-electron ions in C_{3h} symmetry; m, magnetic dipole transition; e, electric dipole transition.

Chapter 3

SPECTRAL HOLE BURNING

A short, general description of hole burning will be given in this chapter with a particular emphasis on saturation holes and long lived holes in rare earth solids. The latter parts of this chapter will focus on an approximate calculation of the parameters one would measure in $Eu(OH)_3$ using hole burning techniques and a short description of homogeneous line width measurements.

When a spectral line is inhomogeneously broadened, and sufficient electromagnetic power is supplied at a single frequency to cause saturation, only those energy levels at the resonant laser frequency will be saturated. A 'hole' appears in the inhomogeneous line.

On the other hand, in a homogeneously broadened line, all energy levels are affected immediately by the saturating electromagnetic power, the intensity falls throughout the line, and no hole is produced.

The atoms or ions in a liquid or solid interact strongly with one another and with vibrational modes. Thus a saturation hole disappears very quickly because of the relatively rapid relaxation rates frequently encountered in solids. The density which is obtainable in a solid is an

advantage however. Nonlinear effects, such as hole burning, scale linearly with the density which should mean an increase in hole burning efficiency. These same nonlinear interactions scale as the fourth power of the dipole moment which is typically much smaller in many solids than it is in gases. This combination, and the relatively rapid relaxation rates in many solids, limits the use of saturation hole burning in solid materials. It does not limit hole burning in general, however, because a saturation hole is not the only kind of hole that can be burned.

Hole burning in solids is a result of a variety of different mechanisms, depending on the particular solid. A list of some of these mechanisms should include photophysical modification[17], photochemistry[18], metastable population storage[19], two level saturation[20], and optical pumping of nuclear hyperfine populations[21,22]. In solids, one or more of the above may be present but it is the last one which is responsible for long lived holes in rare earth materials.

Hole Burning in Rare Earths

Two level saturation hole burning in rare earth solids requires the use of two lasers. The strong pump laser interacts with the two level system such that the population in the ground and excited states depends on the pump laser intensity as well as the dipole coupling between the levels in the particular system. When a weak probe laser interacts

with the same two level system it will feel the full absorbing power of the inhomogeneous profile unless it is interacting with the ions that are also resonant with the strong pump beam. In that case, the absorption is saturated by the pump beam so the sample appears to be more transparent. A hole is then detected as the probe frequency is scanned through the inhomogeneous absorption profile. Saturated absorption spectroscopy of this type can be used to measure the homogeneous linewidth in rare earth compounds. These measurements and their limitations will be addressed later in this chapter.

In the long lived hole burning process in rare earth solids, population is selectively removed from the ground state level associated with an inhomogeneously broadened transition. This selectivity is in most cases much narrower than the inhomogeneous width of the optical transition, and the ground state hyperfine level population is redistributed as a result of the optical pumping. As these resonant ground state levels are depopulated, the nonresonant level populations are enhanced by the transfer of population between the hyperfine levels during the pumping process. Now transitions from the depleted regions in the spectral line will show holes corresponding to the energy level separations of the excited state hyperfine levels. Simultaneously, antiholes or increased spectral absorption

will appear at energies corresponding to the sum and difference combinations of ground and excited state hyperfine splittings.

By using this method, spectral resolution within the inhomogeneously broadened spectral line is achieved. This is important, because the observed hyperfine splittings are usually much less than the Full Width at Half Maximum, FWHM, of the inhomogeneously broadened line. In other words this is a solid state analogue of Doppler-free spectroscopy in atomic physics.

Hole burning has been of particular interest in Eu^{3+} compounds because as Elliott[23] pointed out there are some major experimental difficulties in doing conventional nuclear magnetic resonance, NMR, and nuclear quadrupole resonance, NQR, experiments on this particular ion. Nuclear resonance is usually observed only in materials which are diamagnetic or very weakly paramagnetic. In paramagnetic ions, the internal field resulting from the electrons creates a field at the nucleus which may be of the order of a million gauss. This is greater than any external field that can be applied in a nuclear resonance experiment and for this reason no direct measurements of nuclear moments by nuclear resonance have been possible in the rare earths, as they do not form diamagnetic compounds.[24] Nuclear magnetic moments can be determined from the hyperfine splittings measured in electron paramagnetic resonance

experiments, but moments determined in this way depend on an estimate of the average $\langle r^{-3} \rangle$, where r is the radius of the 4f electron.

Europium does have a non-degenerate electronic ground state which produces no magnetic field at the nucleus, and since conventional NMR and NQR cannot be used because of the limited sensitivity. The development of narrow linewidth, (1MHz), tuneable lasers has provided another means for making these measurements. Ground and excited state hyperfine splittings[21,25], Stark effects[26], and Zeeman effects[27] have all been measured using hole burning techniques. Through the use of hole burning, the hyperfine structure of the $^1D_2 - {}^3H_4$ transition in $Pr^{3+}:LaF_3$[21,25], $Pr^{3+}:LaCl_3$[28], and $Pr^{3+}:LaBr_3$[29] have been investigated. Since that time, hole burning and optically detected nuclear quadrupole resonance, ODNQR, techniques have been used to measure the quadrupole splittings in EuP_5O_{10}[30] and $YAlO_3:Eu^{3+}$.[31] Since the rare earth optical absorption lines are so narrow due to lanthanide contraction, they are the most attractive candidates to detect the hyperfine structure by the use of direct spectroscopy. Except for two isolated examples this has not been possible. It is possible in Ho^{3+} because of the lucky coincidence of three things, a very small inhomogeneous linewidth, a very large magnetic nuclear moment, and the existence of only one isotope, ^{165}Ho.[32] It

has also been observed in 0.01% $CaF_2:Pr^{3+}$ which has a large hyperfine splitting constant of 2.7 GHz and a narrow inhomogeneous width of 650 MHz.[33]

Recently spectral hole burning has also been used in $EuVO_4$[34] to identify the hyperfine splittings of perturbed sites in this material, and it has also shown a usefulness as a very sensitive identification of the particular perturbations of some of the individual sites.

Hole burning measurements of the hyperfine splittings in Pr^{3+} and Eu^{3+} rare earth compounds have complemented the electron paramagnetic resonance measurements obtained in other materials. These experimental measurements have also added a great deal to the understanding of the many contributions which affect the magnitude of the quadrupole tensor in the ground states and the excited states of rare earth materials. In europium compounds this is particularly interesting because of Elliott's prediction[23] that the ground state nuclear quadrupole tensor would be anomalously small.

Nuclear Quadrupole Hamiltonian

The large difference in magnitude of the quadrupole tensor between $^5D_0$ and $^7F_0$ states[30,31] is attributed to the contribution to the electric field gradient of two important mechanisms. Since no first order quadrupole coupling exists for a pure J = 0 level, the observed field gradients are due to admixtures of excited states into the $^7F_0$ and $^5D_0$ wave

functions and a contribution caused by the crystalline lattice.

The two contributions to the quadrupole splitting, are of opposite sign,[35,36] and are from the excited states of the $4f^6$ configuration. The contribution for $^5D_0$ which results from the $^5D_2$ level, with an energy denominator of 4230 cm^{-1} in the perturbation expansion, is smaller than the contribution to $^7F_0$ from the $^7F_2$ state which has an energy denominator of 1151 cm^{-1}. So the smaller quadrupole coupling for $^7F_0$ is a result of the lattice contribution which nearly cancels the contribution due to the $^7F_2$ admixture.

To derive an expression for the different contributions to the quadrupole tensor, the quadrupole splittings are first described by the spin Hamiltonian:[24]

$$H = P[I_z^2 - I(I + 1)/3 + \eta(I_x^2 + I_y^2)/3]$$

where each P is proportional to the respective quadrupole moment of each of the two europium isotopes. The asymmetry parameter, $\eta = (V_{xx} - V_{yy})/V_{zz}$, has a value between 0 and 1. For C_{3h} site symmetry, as in $Eu(OH)_3$, $V_{xx} = V_{yy}$ and $\eta = 0$. The spin Hamiltonian is then

$$H = P[I_z^2 - (1/3)I(I + 1)]$$

where $$P = \sum P_i = P_{4f}^{(1)} + P_{pq} + P_{lat} + P_{4f}^{(2)}.$$

In the above expression, each of the contributions to the total quadrupole coupling constant P will be explained in the order in which they appear. $P_{4f}^{(1)}$ is the first order quadrupole term which is the dominant term observed in nuclear electric quadrupole resonance experiments. P_{pq} is a pseudoquadrupole interaction which is a magnetic effect unrelated to the nuclear quadrupole moment. This term is proportional to the square of I·J, so experimentally it cannot be distinguished from the quadrupole effect. Fortunately however this interaction is negligibly small in $Eu(OH)_3$. P_{lat} is the contribution caused by the crystalline lattice. The external lattice charges tend to induce a polarization of the closed electronic shells which in turn leads to an enhancement of the quadrupole moment. The last term, $P_{4f}^{(2)}$, is a result of the distortion of the electronic charge cloud of the J=0 state with admixtures of the J=2 states through interactions of the crystal field.

The first order 4f term is given by[37]

$$P_{4f}^{(1)} = - [3e^2Q/4I(2I - 1)] (1 - R_Q) [3J_z^2 - J(J + 1)] \times \langle r^{-3} \rangle_{4f} \langle J||\alpha||J \rangle .$$

The quantity $\langle J||\alpha||J \rangle$ results from application of the Wigner-Eckart theorem to evaluate the crystal field interaction by an operator equivalent, and $\langle r^{-3} \rangle_{4f}$ is the actual expectation value of r^{-3} for 4f electrons in the ion.

The expectation value of the quadrupole inverse radius cubed, $\langle r^{-3} \rangle_Q$, is given by

$$\langle r^{-3} \rangle_Q = (1 - R_Q) \langle r^{-3} \rangle_{4f},$$

where R_Q is the atomic Sternheimer factor. This first order term, $P_{4f}^{(1)}$, is zero, because there can be no quadrupole splitting for a $J = 0$ level.[24]

The pseudoquadrupole interaction constant, P_{pq}, has been estimated by several authors to be less than 0.052 MHz[36,37] which is an entirely negligible contribution compared to the last two terms in the sum.

The quadrupole coupling constant can now be written as the sum of just two terms

$$P = P_{lat} + P_{4f}^{(2)}.$$

The important thing to notice is that these two parts contribute to the nuclear electric quadrupole coupling constant with different signs.

$$P_{lat} = -[3Q(1 - \gamma_\infty) A_2^0] / I(2I - 1)$$

$$P_{4f}^{(2)} = [6e^2 Q A_2^0 \langle r^2 \rangle_{4f}(1-\sigma_2)\langle r^{-3} \rangle_{4f}(1-R_Q) \times |\langle 20||\alpha||00\rangle|^2] / I(2I-1)(E_{20}-E_{00})$$

Here γ_∞ is the Sternheimer factor for the lattice. In the ground state where the antishielding parameter γ_∞ is large, $\gamma_\infty = -80$,[36] the contribution from the lattice nearly cancels the second order contribution from $P_{4f}^{(2)}$. In the excited state $^5D_0$, γ_∞ should be small or even equal to 1,

so that the quadrupole splitting will only be the result of the second order contribution.

Estimate of Quadrupole Splitting in $Eu(OH)_3$

Using parameters from Cone and Faulhaber[12] and the γ_∞ and σ_2 values for Europium Ethyl Sulfate,[37] where measurements of these values have been made, one can calculate an approximate quadrupole coupling constant P for the two isotopes of Eu^{3+} where each of the isotopes have a nuclear spin of I = 5/2.

$$(3/5)\ A_2^0 \langle r^2 \rangle = E_{10} - E_{11} = 101.5\ cm^{-1}$$

$$A_2^0 \langle r^2 \rangle = 169.2\ cm^{-1}$$

$$\langle r^{-3} \rangle_{4f} = 7.41\ a_0^{-3}$$

$$(1 - \sigma_2) = 0.27$$

$$A_2^0 \langle r^2 \rangle (1 - \sigma_2) = 45.7\ cm^{-1}$$

$$A_2^0 = 193.4\ cm^{-1}\ a_0^{-2}$$

$$(1 - \gamma_\infty) = 81$$

$$E_{20} - E_{00} = 1151\ cm^{-1}$$

For the ground state $^7F_0$ this gives

$$P_{lat} = -18.6\ Q\ \ MHz$$

$$P_{4f}^{(2)} = 17.3\ Q\ \ MHz$$

with Q, the quadrupole moment, in barns.

$$P = P_{lat} + P_{4f}^{(2)} = -1.3\ Q$$

which implies a P of -3.2 MHz for ^{153}Eu and -1.2 MHz for ^{151}Eu.

As a first approximation of the excited state, $^5D_0$,

quadrupole coupling constant one can assume $\gamma_\infty = 1$, so that $P_{lat} = 0$. With the energy difference

$$E_{20} - E_{00} = (21455 - 17225)\ cm^{-1}$$
$$= 4230\ cm^{-1}$$

and $$P = P_{lat} + P_{4f}^{(2)}$$

one obtains $P = 0 + 4.71\ Q\ MHz = 4.71\ Q\ MHz$.

The quadrupole moment for ^{153}Eu is Q = 2.45 barns and for ^{151}Eu it is Q = 0.95 barns[38], so the predicted quadrupole coupling constants are P = 11.5 MHz and P = 4.5 MHz for the 153 isotope and the 151 isotope respectively.

It should be noted that this is just an approximate calculation because the parameters $\langle r^{+2}\rangle, \langle r^{-3}\rangle_{4f}, (1-\gamma_\infty)$, and $(1 - \sigma_2)$ are by no means the same in the Ethyl Sulfate as they are in $Eu(OH)_3$. This is especially true for γ_∞ in the excited state because no measurements or estimates exist. The agreement is very good, however, because as we shall see the measured values for these two constants using hole burning techniques are P = 11.6 MHz for ^{153}Eu and P = 4.5 MHz for ^{151}Eu as discussed in the last section of chapter 6.

Hole Burning Measurement of Dephasing Time

Spectral hole burning can also be used to measure the optical dephasing time or transverse relaxation time T_2. In this method, the sample is prepared by irradiation at a single frequency, which induces a polarization in the sample with a width H, where $H = 2(\Delta\omega_H + \Delta\omega_I)$. The observed hole

width is then given by a convolution of the homogeneous linewidth, $\Delta\omega_H$, and the instrumental linewidth, $\Delta\omega_I$. For CW dye lasers the instrumental linewidth $\Delta\omega_I$ is the bandwidth of the laser itself, approximately 1 MHz. So for measurements of hole widths greater than 5 or 10 MHz, deconvolution is not necessary, and the instrumental width can be considered negligible. The dephasing time is then given by $T_2 = (\pi\Delta\omega_H)^{-1} = (2/\pi H)$. This is strictly valid in the limit where the laser power goes to zero, but it is often difficult to make measurements which are reliable for the following reasons.

In the low power limit, the hole will still be slightly power broadened and only in the limit of zero power, no light, will the hole display the true homogeneous width. The most important difficulty, however, is the broadening of the hole by time dependent interactions. This is important because spectral diffusion due to radiative and nonradiative transfer will affect the hole depth and width on time scales which may be faster than the time required to measure the width or depth of a hole. One solution involves the use of two lasers, one to burn the hole and the other to monitor or read the spectrum as a function of time. In some cases, this technique has been successful[39], but in most cases, it only gives a lower limit on the optical dephasing time T_2.

In any case, if a hole width, H, can be measured, $T_2 \geq (2/\pi H)$ is always true.

Chapter 4

OPTICAL PHASE SWITCHING

Since the discovery of the photon echo[40] in ruby, techniques such as free induction decay[41], optical hole burning[42], laser frequency switching[43], and sample frequency switching[44] have all been used to measure the optical dephasing time in a variety of materials. With some restrictions these methods of transient spectroscopy can all be used to measure the dephasing time in a rarefied gas where the optical dephasing time, T_2, is simply related to the spontaneous emission time T_1, $T_2 = 2T_1$. In stoichiometric solids, however, the atoms or ions strongly interact with neighboring atoms or ions and the rest of the environment. This affects the coherence or dephasing time T_2 such that, at low temperatures, it is usually much less than the diagonal lifetime T_1. So the interest in the optical dephasing time is to better understand the interactions which can lead to a lengthening or shortening of this coherence time. This understanding is an important step in the development of lasers and optical devices in general.

Single Phase Switch

Optical phase switching[45] is a new and powerful approach to coherent transient spectroscopy. By rapidly changing the phase of the laser light passing through an absorbing medium, the phase of the laser polarization is switched relative to the sample polarization which was established in the sample before the phase switch. Once the phase switch has taken place, the sample and the laser are again at the original frequency and as the sample relaxes back into equilibrium, a transient signal is detected.

First consider the laser sample interaction as a preparation stage where the polarization of the sample is driven by the laser. After the phase switch, the small field emitted by the sample propagates collinearly with the laser beam at the same frequency. This results in homodyne mixing of the sample signal with the laser beam which serves as the local oscillator.

Genack et al,[45] in a calculation of the sample response to a sudden phase shift, expressed the laser field whose phase is instantaneously shifted by an amount ϕ at t=0 as

$$E(t) = 2E\sin[\omega t+\phi(t)] = -i[E^{+}e^{i\omega t}-E^{-}e^{-i\omega t}]$$

with

$$E^{\pm} = \begin{cases} E & ,t<0 \\ Ee^{\pm i\phi} & ,t>0 \end{cases} \qquad 2.1$$

One must then solve the optical Bloch equations for the